Contribution to the numerical and experimental study of gravity capillary waves in a hydraulic channel: the influence of a sheared velocity profile

A. YOUNSI, M. BOUHADEF and T. GUENDOUZEN-DABOUZ
Laboratoire GIENA, Department of Hydraulics, Faculty of Civil Engineering
University Houari Boumediene of Science and Technology (USTHB)
B.P. 32 Bab-Ezzouar, 16111 Alger
ALGERIA

Abstract: - The numerical and experimental two-dimensional free-surface flow of a viscous incompressible fluid moving in a channel is examined. Special attention is given to the propagation of gravity-capillary waves, on the surface of a finite depth hydraulic channel. The classical governing Navier Stokes equations are written in their non dimensional form with the corresponding boundary conditions including the surface tension coefficient •. One explicitly shows, in addition to the Froude number, the influence of the velocity, and its gradient at the free-surface, on the characteristics of the waves.

Key-Words: Gravity capillary waves – Free surface – Wave propagation – Hydraulic channel – Laboratory experiments

1 Introduction

The undulatory movements, in a non homogeneous fluid, owe their existence to the gravity and a stratification of the density. The oscillatory nature of these waves is due to the force of recall which is exerted on a fluid particle when an external force tends to draw it aside from its equilibrium position. The gravity waves, which also appear on the surface of a liquid, are due to the sharp variation of density (there is a discontinuity since the densities of water and the air, on both sides of the interface, are very different). They are said, in this case, "surface waves" and are an example of standing waves. They can be produced, for example, by the presence of a deformation on the bottom of a channel. The problem of their modelling is still of topicality, within sight of the difficulties encountered in its resolution in the assumption of an inviscid fluid. Several attempts were carried out, like those of Lamb [13], Euvrard [8], Forbes et al. [9], Cahouet [6], Bouhadef et al. [4] and Younsi et al. [17] to quote only some. In order to compare the influence of a sheared velocity profile, due to the existence of the viscosity, with an inviscid theoretical velocity profile, we can also tract, at a constant speed, the disturbing obstacle in a fluid otherwise at rest. For that, an experimental special device is designed. The waves observed, if one moves with the obstacle, will be thus steady and their characteristics (amplitude, wavelength) accessible by measurement via a photographic system for example.

Let us note that, to our knowledge, few works are devoted to the problem of the influence of the velocity profile on the propagation of gravity waves, especially their wavelength as in atmospheric waves [16].

2 Mathematical formulation

The starting point of the derivation is the unsteady Navier-Stokes equations for viscous incompressible flow velocity $\vec{\bar{V}} = (\bar{u},\bar{v})$ in two-dimensional cartesian coordinates in a hydraulic channel, whose free-surface is disturbed by the presence of an obstacle or an external action. One takes into account, in addition to the gravity forces, the surface tension.

The $\bar{x}$ and $\bar{y}$ coordinates are horizontal and vertical, respectively, with the origin located at the upstream bottom (Figure 1).

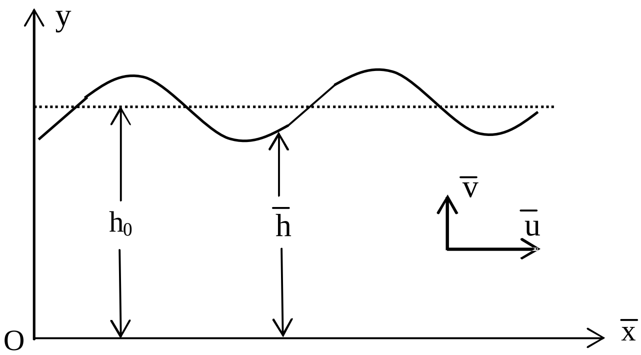

Figure 1

$$\frac{\partial \bar{u}}{\partial \bar{t}} + \bar{u}\frac{\partial \bar{u}}{\partial \bar{x}} + \bar{v}\frac{\partial \bar{u}}{\partial \bar{y}} = -\frac{1}{\rho}\frac{\partial \bar{p}}{\partial \bar{x}} + \nu\Delta\bar{u} + g_x$$

$$\frac{\partial \bar{v}}{\partial \bar{t}} + \bar{u}\frac{\partial \bar{v}}{\partial \bar{x}} + \bar{v}\frac{\partial \bar{v}}{\partial \bar{y}} = -\frac{1}{\rho}\frac{\partial \bar{p}}{\partial \bar{y}} + \nu\Delta\bar{v} + g_y$$

$$\mathrm{div}\,\vec{\bar{V}} = 0$$

with the classical boundary conditions:

$$\bar{u}(0) = \bar{v}(0) = 0$$

$$\bar{v}(\bar{h}) = \frac{\partial \bar{h}}{\partial \bar{t}} + \bar{u}\,\frac{\partial \bar{h}}{\partial \bar{x}}$$

$$P(\bar{h}) = -\sigma \frac{\partial^2 \bar{h}}{\partial \bar{x}^2} \;/\; \left[1 + \left(\frac{\partial \bar{h}}{\partial \bar{x}}\right)^2\right]^{3/2}$$

where $\bar{P}$ is the relative pressure and • the surface tension coefficient.

We neglect the interaction between turbulence and the wave phenomena.

It is known that if f is the frequency of the waves and ν the kinematic viscosity of the fluid, the non dimensional thickness of the boundary layer is of order $(\nu/f)^{1/2}$. It is assumed that the non dimensional number $(f\, h_0^2/\nu)$ is very large so that one can neglect the influence of the boundary layer on the propagation of the waves. Indeed, the non stationary effects are confined, in the case of great frequencies, in a layer of thickness very small comparatively to the boundary layer thickness.

As in [4], we write:

$(\bar{u}, \bar{v}, \bar{P}, \bar{h}) = (U_0, 0, P_0, h_0) + (\bar{u}_1, \bar{v}_1, \bar{p}_1, \bar{h}_1)$

where $U_0(\bar{y})$, $P_0 = \rho g(ho - \bar{y})$ are the velocity and pressure profiles of the basic steady undisturbed flow.

By introduction of the reference variables, the equations are written in a non dimensional form and the following parameters are thus defined: the Froude number $F = U_d/(gh_0)^{1/2}$, the wave number $\varepsilon = 2\pi h_0/\lambda$, the phase velocity•β and the Bond number $B = \sigma/\rho g h_0^2$.

If one assumes sinusoidal waves [15], the non dimensional expressions of the pressure and the velocity components can be written in the following form:

$(p, u, v) = R_e\{[P(y), U(y), V(y)] \exp [2i\pi(x-\beta t)]\}$

where $P(y)$, $U(y)$ and $V(y)$ are complex variables and R_e designates their real part.

The substitution of these relations in the Navier-Stokes equations and the boundary conditions leads to the following differential equation for the pressure $P(y)$:

$$P'' - [2F / FU - \beta)]\, P' - \varepsilon^2 P = 0 \qquad (1)$$

$$P'(0) = 0 \qquad (2)$$

$$P'(1) = \{\varepsilon^2 [\beta - F\, U(1)]^2 / (1 + B\, \varepsilon^2)\}\, P(1) \qquad (3)$$

where U(y) is the non dimensional velocity profile, U' its first derivative. The determination of the phase velocity β leads to the resolution of an eigenvalues problem. To compute the pressure field, an additional condition related to the wave amplitude and the flow disturbance discharge is necessary:

$$P(1) = (1 + B\, \varepsilon^2) / [\beta - F\, U(1)] \qquad (4)$$

3 Theoretical results

2.1 Analytical resolution

For very small Froude numbers, analytical solutions of the equation (1) can be sought in the form [17]:

$P = P_0 + F\, P_1 + F^2 P_2 + \ldots\ldots.$

$\beta = \beta_0 + F\, \beta_1 + F^2\, \beta_2 + \ldots\ldots$

We consider the following theoretical velocity profiles:

1: U(y) = 1 (inviscid fluid)

2: U(y) = 2y

3: $U(y) = 3y - (3y^2/2)$ (parabolic velocity profile)

4: $U(y) = 6/5\, y^{1/5}$ (turbulent velocity profile)

5: $U(y) = 1.15 - 0.38\,(1-y)^2 - 0.771\,(1-y)^{32}$ (turbulent velocity profile suggested by Pai [14])

We give, as example, the expressions for the second sheared linear velocity profile:

$\beta_0^2 = (1+B\varepsilon^2)\,(\tanh\varepsilon / \varepsilon)$;

$\beta_1 = 2 - (\tanh\varepsilon / \varepsilon)$;

$\beta_2 = (1/2\beta_0)\,(\tanh\varepsilon / \varepsilon)^2$

2.2 Numerical resolution

When the Froude number F is not small any more, the development would require a high number of terms. We thus solve the system of equations by using a finite 1D element method with an iterative process to compute ε.

The figure 2 shows dispersion diagrams for 4 velocity profiles:

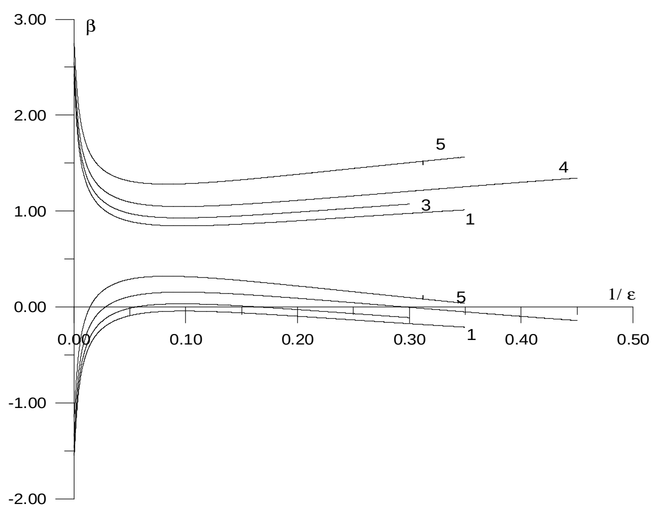

Figure 2

One notes, for all the velocity profiles, the existence of two points, on the horizontal axis, for which the phase velocity β is null. These standing waves correspond to capillary waves (small wavelength and negative group velocity; propagation in the inverse direction of the

flow) and gravity waves (larger wavelength and positive group velocity; propagation in the direction of the flow). The same iterative process, associated to the finite 1D element method, allows us to determine, for a given velocity profile U(y) and a Bond number B, the wavelength variation of standing waves with the Froude number (Figure 3).
For each velocity profile, the lowest part of the curve corresponds to capillary waves whereas the upper part is relative to gravity waves.
Standing waves do not exist for any Froude number; the limiting Froude number, depending on the velocity profile, is inversely proportional to the velocity on the free-surface.
One notes that these curves, for a given Bond number, respect the hierarchy according to the value of the velocity at the free-surface. For a given Froude number, the highest wavelength of the gravity waves corresponds to the velocity profile having the highest free-surface velocity and conversely for the capillary waves.

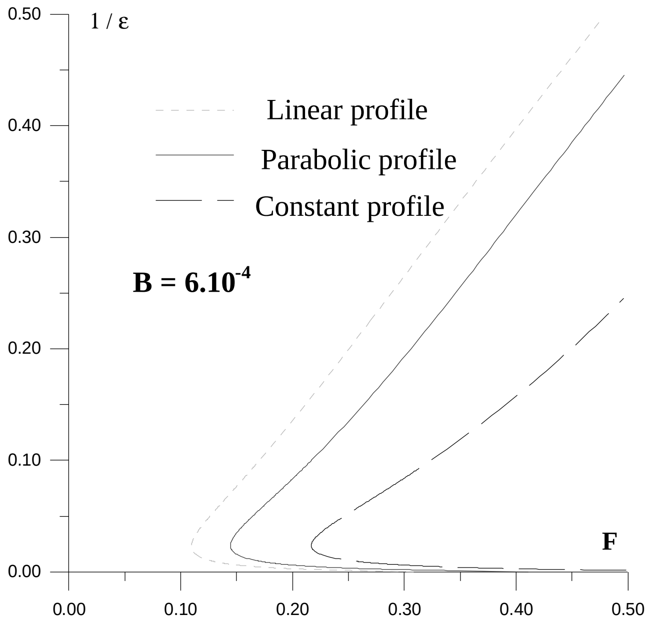

Figure 3

This established result reported, one proposes to check if that it is mainly the velocity on the free-surface which controls the propagation of gravity and capillary waves. To do that, one considers another theoretical velocity profile having the same value of the velocity at the free-surface as the basic profile (parabolic). Such a velocity profile has the following expression: $U = \frac{3}{2}\sqrt{y}$ to verify the flow discharge condition $\int U dy = 1$.
One notes that the evolution of the non dimensional wavelength $1/\varepsilon = \lambda/2\bullet ho$ versus the Froude number is identical for the two profiles for the capillary waves whereas a small difference exists, beyond a certain value of the Froude number, for gravity waves (Figure 4).
For moderated Froude numbers, the waves induced, for example, by an obstacle lying on the bottom of a hydraulic channel, have a wavelength which is about the thickness of the fluid layer. It follows that the relative wave number ε has an approximate value of•6. For the capillary waves, ε is still much larger. It is thus very indicated to make a development of the analytical relations for great values of ε. Following [17], we have, with z = y-1:

$$\beta \approx [(1/\varepsilon) + B\varepsilon]^{1/2} + F\,U(0) - (F/2\varepsilon)\frac{dU}{dz}(0)$$

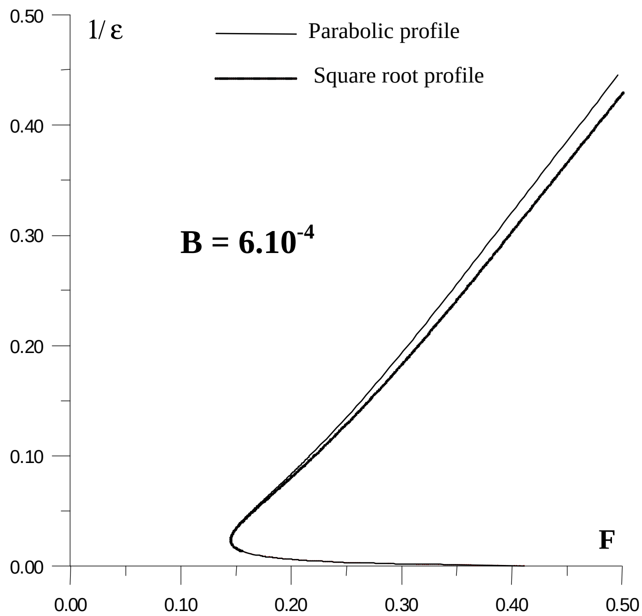

Figure 4

The wavelengths of the standing waves are thus the solutions of:

$$(1/\varepsilon^2)\,[1+F^2U(0)\frac{dU}{dZ}(0)] - \{[F^2\,U^2(0)]\,/\varepsilon\} + B = 0 \quad (5)$$

We represent, on the figure 5, the curves corresponding to the roots of this equation for the two cases considered, namely the parabolic profile, for which $\frac{dU}{dz}(0) = 0$, and the square root profile for which $\frac{dU}{dz}(0) = 3/4$. It is noted that the higher parts (gravity waves) of these 'asymptotic' curves, built from the solutions of the equation (5), and for a Bond number of 6.10^{-4}, do not overlap completely beyond the Froude number of about 0.2.
The two profiles differ by the value of their velocity gradient at the free-surface. This parameter seems to be

another influencing factor, as well as the velocity on the free-surface, in the estimation of the wavelength gravity waves.

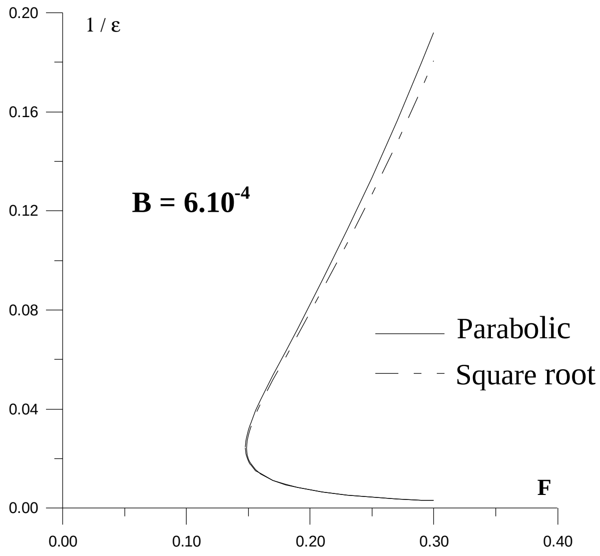

Figure 5

To confirm this result, one must consider another velocity profile which has the same value of the velocity and the same value of the velocity gradient on the free-surface as the parabolic velocity profile. The selected velocity profile is: $U = \frac{15}{2} y^4 - 18\, y^3 + 12\, y^2$

In the approximation which led to the establishment of equation (3), these two profiles lead to identical curves. One represents, on the figure 6, the curves obtained by the numerical method. It clearly appears a divergence of the curves for the gravity waves only. This indicates the existence of another parameter intervening, in addition to both others already mentioned.

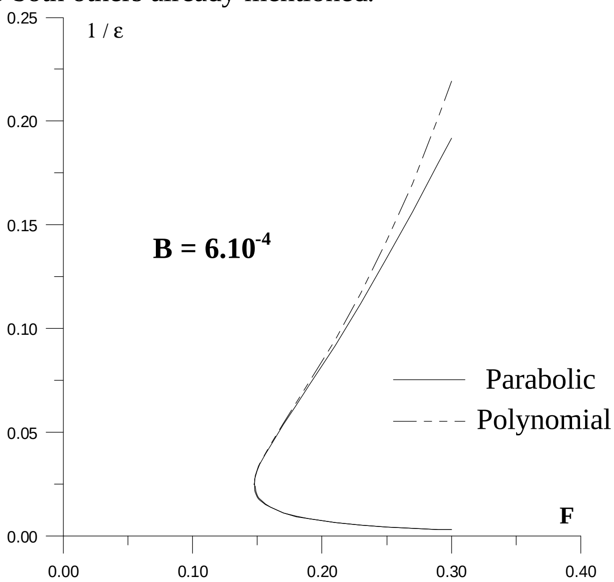

Figure 6

4 Experimental study

This study follows that carried out by the author; the experiments were undertaken in the same hydraulic channel. The ripples are created by the disturbance of the free-surface by a liquid level recorder with point (photo 1). The gravity waves, on the other hand, are generated by a triangular obstacle with a maximum length of 60 cm, a width of 30 cm and heights ranging between 5 cm and 10 cm (photo 2).

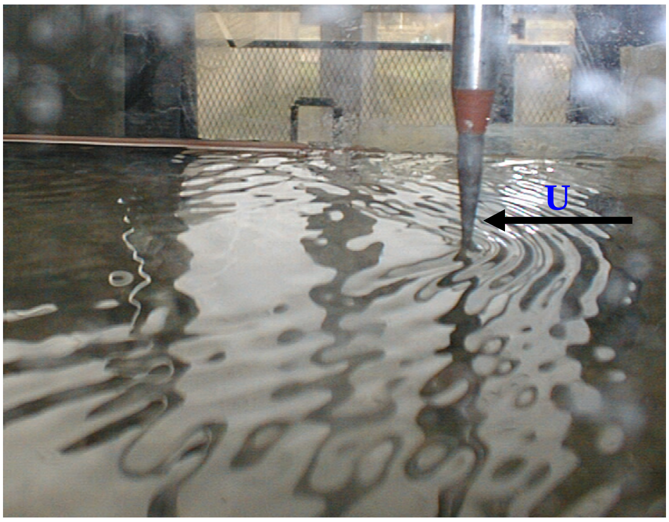

Photo 1

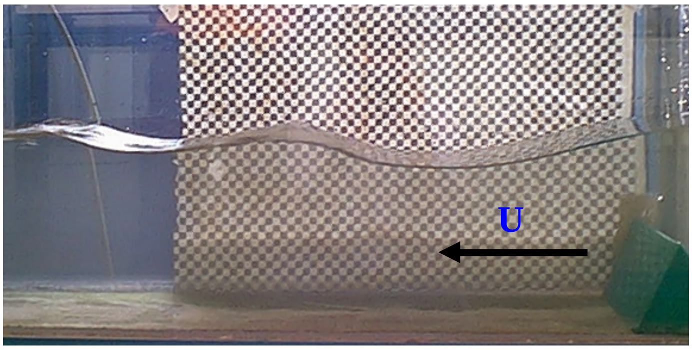

Photo 2

The amplitude of the capillary standing waves, which occur upstream of the obstacle, is lower than 5 mm and decreases while moving away from the obstacle. The number of crests which could be counted is limited (4 to 8). To decrease the measurement error, one takes into account several wrinkles. The space dimension is appreciated by means of a rule, a slide caliper in our case.

The wavelengths of the gravity waves are larger than those of the capillary waves. The wavelength is measured by using a camera. When the system of waves is established with their maximum amplitudes, one carries out the acquisition of the photography of the free-surface.

The figure 7 represents the experimental results obtained for the capillary waves with h_0 = 15 cm compared to those numerically computed.

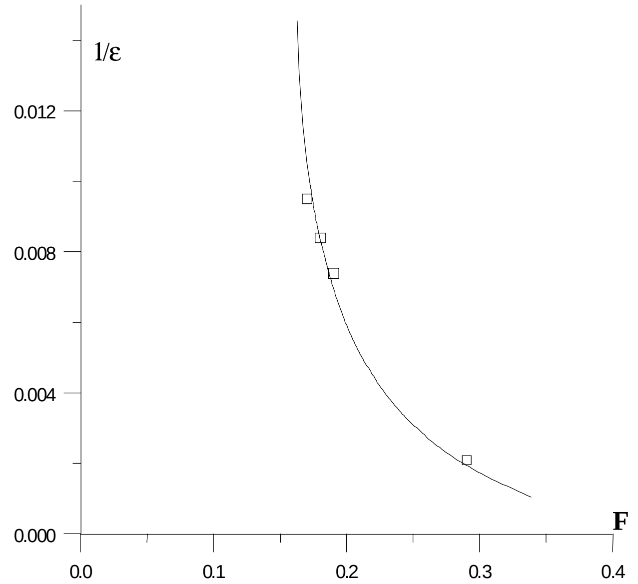

Figure 7

The figure 8 represents the experimental results obtained for the capillary waves with h_0 = 18 cm compared to those given by the numerical method.

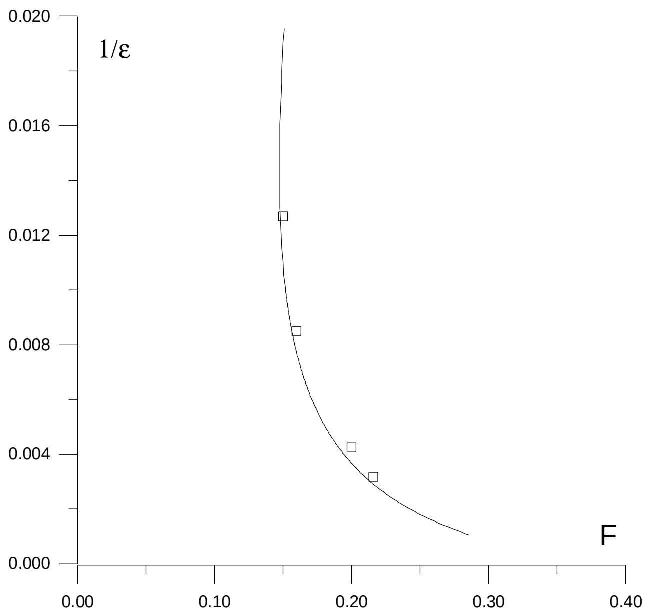

Figure 8

The figure 9 represents the evolution of the wavelength of gravity waves with the Froude number.

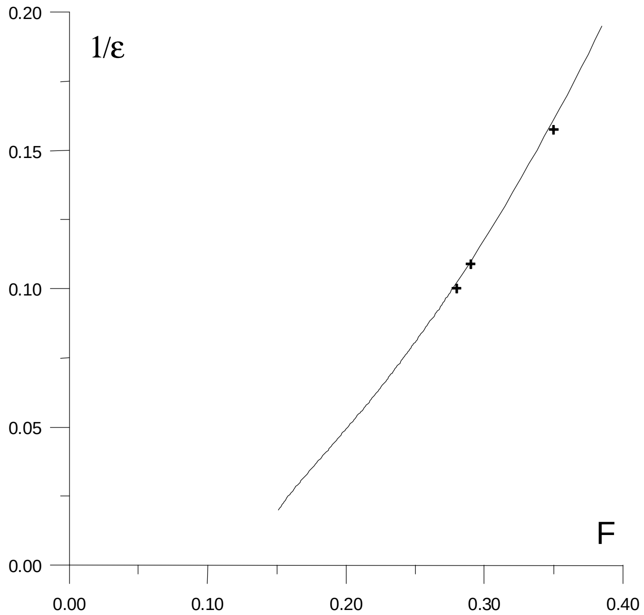

Figure 9

A quite good agreement is observed for both capillary and gravity waves as we can note it on the figure 10 corresponding to h_0 = 18 cm.

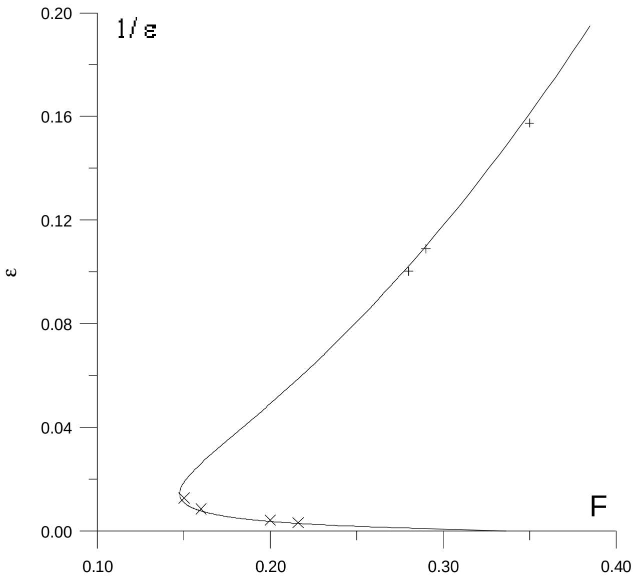

Figure 10

We have remarked that for a Froude number equal to 0.11 and h_0 = 18 cm, the free-surface remains plane in spite of the presence of the obstacle in accordance with the theory.

4 Conclusion

The theoretical curves giving the wavelength evolution of the capillary standing waves, with the Froude number, show that neither the free-surface velocity gradient, nor the profile shape have a notable influence on the variation of their wavelength. Only the velocity on the free-surface and obviously the Bond number control the variation of the capillary wavelength of wrinkles with the Froude number. For the gravity waves, on the other hand, the form of the velocity profile strongly intervenes, especially when the Froude number is not small.

References:

[1] M. Amara et M. Bouhadef. A new approach of numerical modelling of 2D surface waves induced by an obstacle. *Computer Meth. and Water Ress*. C. M. P., 1991.

[2] K.J. Bai. A localized finite element method for steady two dimensional free-surface flow problems. *1st Internat. Conf. Numer. Ship Hydrodyn*. Gaithersburg, Maryland, 209, 1975.

[3] M. Bouhadef, B. Bauche, J.-L. Peube. Structure de l'écoulement à surface libre derrière un obstacle noyé au fond d'un canal. *C.R.Acad. Sci. de Paris*. 292, 1981.

[4] M. Bouhadef, J.-L. Peube. Propagation des ondes superficielles de faible amplitude aux petits nombres de Froude dans un écoulement à gradient vertical de vitesse. Journal. Méc. Théor. et Appli. Vol. 7, n°1, 1988.

[5] Y.Z. Boutros, M.B. Abdelmalek et S.Z. Masoud. Linearized solution of a flow over a non uniform bottom. *J. Comp. Appl. Math*., 16, 105, 1986.

[6] J. Cahouet et M. Lenoir. Résolution numérique du problème non linéaire de la résistance de vagues bidimensionnelle. *C.R.Acad. Sci. de Paris*. 297, 1983.

[7] De Gennes P. G., Raphael E. Capillary gravity waves caused by a moving disturbance: wave resistance, Physical review, vol. 53, 4, pp 3448-3455, 1996.

[8] D. Euvrard. Sur la possibilité d'une résolution numérique directe du problème de Neumann-Kelvin, par introduction d'une perturbation singulière. *C.R.Acad. Sci. de Paris*. 262, 1976.

[9] Forbes L.K. and Schwartz L.W. Free surface flow over a semicircular obstruction. J. Fluid Mech. 114, 299, 1982.

[10] A.S. Gazdar. Generation of waves of small amplitude by an obstacle placed on the bottom of a running stream. *J. Phys. Soc. Japan* 34, 2, 530, 1973.

[11] A.F. Ghaleb et A.Z. Hefni. Wave free, two-dimensional gravity flow of an inviscid fluid over a bump. *J. Mec. Theor. Appl*., 6, 4, 1987.

[12] C.H von Kerczek, N. Salvesen. Numerical solutions of two dimensional nonlinear wave problems. *10th Symp. Naval Hydrodyn*., 649, M.I.T., Cambridge, 1974.

[13] H. Lamb. Hydrodynamics. *Cambridge University Press*, 1932.

[14] S.I. Pai On turbulent flow between parallel plates A.S.M.E., 20, pp 109-1114, 1952.

[15] M. Souli et J.P. Zolesio. Finite element method for free-surface flow problems. *Comput. Methods Appl. Mech. Engrg*. 129, 1996.

[16] A.C.M. Teixiera, P.M.A. Miranda. *The effect of wind shear and curvature on the gravity wave drag*. J. Atmosph. Sc., 61, 2638, 2004.

[17] A. Younsi, M. Bouhadef. Contribution à l'étude des ondes gravito-capillaires dans un canal hydraulique. 2ème Congrès de Mécanique, Faculté des Sciences Ain Chok. Casablanca, 231, 1995.

[18] J.V. Wehausen, E.V. Laitone. Surface waves. Handb. Phys., 9, Springer Verlag, 1960.